Appl. Environ. Microbiol. doi:10.1128/AEM.00757-16

Regulation of polyhydroxybutyrate synthesis in the soil bacterium *Bradyrhizobium diazoefficiens*

J. I. Quelas[a], S. Mesa[b], E. J. Mongiardini[a], D. Jendrossek[c] and A. R. Lodeiro[a#]

Laboratorio de Interacciones entre Rizobios y Soja (LIRyS) IBBM-Facultad de Ciencias Exactas, UNLP-CONICET (Argentina)[a], Department of Soil Microbiology and Symbiotic Systems, Estación Experimental del Zaidín, Consejo Superior de Investigaciones Científicas (CSIC), Granada (Spain)[b], Institute of Microbiology, University Stuttgart, Stuttgart, (Germany)[c].

Running Head: Regulation of PHB cycling in *Bradyrhizobium diazoefficiens*

[#]Address correspondence to Anibal R. Lodeiro, lodeiro@biol.unlp.edu.ar.

ABSTRACT

Polyhydroxybutyrate (PHB) is a carbon and energy reserve polymer in various prokaryotic species. We determined that, when grown with mannitol as the sole carbon source, *Bradyrhizobium diazoefficiens* produces a homopolymer composed only of 3-hydroxybutyrate units (PHB). Conditions of oxygen limitation (such as microoxia, oxic stationary phase and bacteroids inside legume nodules) were permissive for the synthesis of PHB, which was observed as cytoplasmic granules. To study the regulation of PHB synthesis, we generated mutants in the regulator gene *phaR* and the phasin genes *phaP1* and *phaP4*. Under permissive conditions, mutation of *phaR* impaired PHB accumulation, and a *phaP1*/*phaP4* double mutant produced more PHB than the wildtype, which was accumulated in a single, large cytoplasmic granule. Moreover, PhaR negatively regulated the expression of *phaP1* and *phaP4* as well as of *phaA1*, *phaA2* (3-ketoacyl-CoA thiolase), *phaC1*, *phaC2* (PHB synthases), and *fixK*$_2$ (CRP/FNR-type transcription regulator of genes for microoxic lifestyle). In addition to the depressed PHB cycling, *phaR* mutants accumulated more extracellular polysaccharide and promoted higher plant shoot dry weight and competitiveness for nodulation than the wildtype, by contrast to *phaC1* mutant strains, defective in PHB synthesis. These results suggest that *phaR* not only regulates PHB granules formation by controlling the expression of phasins and biosynthetic enzymes, but also acts as global regulator of excess carbon allocation and symbiosis by controlling *fixK*$_2$.

IMPORTANCE

In this work we investigated the regulation of polyhydroxybutyrate synthesis in the soybean-nodulating bacterium *Bradyrhizobium diazoefficiens* and its influence in bacterial free-living and symbiotic life-styles. We uncovered a new interplay between

the synthesis of this carbon reserve polymer and the network responsible for microoxic metabolism through the interaction between the gene regulators *phaR* and *fixK*$_2$. These results contribute to the understanding of the physiological conditions required for polyhydroxybutyrate biosynthesis. The interaction between these two main metabolic pathways is also reflected in the symbiotic phenotypes of soybeans inoculated with *phaR* mutants, which were more competitive for nodulation, and enhanced dry matter production by the plants. Therefore, this knowledge may be applied to the development of superior strains to be used in improved inoculants for soybean crops.

INTRODUCTION

Bradyrhizobium diazoefficiens is an important soil bacterium that fixes atmospheric N_2 in symbiosis with soybean, a key crop for food production worldwide (1). In addition to its agricultural relevance, *B. diazoefficiens* might have industrial interest because it produces significant quantities of polyhydroxybutyrate (PHB), a polymer that accumulates as granules into the cytoplasm and has potential use as biodegradable plastic (2-6). PHB granules are synthesized as sinks of excess carbon and reducing power, and are used as carbon and energy reserve when bacteria face starving conditions (7). However, this cycle of synthesis and degradation must be regulated because if both pathways occur simultaneously (8), the net result would be consumption of energy and reducing power. The proteins involved in the different steps of the PHB cycle are well-characterized (9-12) and all of them are present in *B. diazoefficiens* (3, 13, 14), but regulation of the cycle in this bacterium was not yet studied. In other rhizobia species, such as *Rhizobium etli* and *Ensifer meliloti*, the gene product of *phaR* (PHA regulator, previously known as *aniA* for anaerobically-induced gene A) was reported to control, at least in part, PHB synthesis (15, 16).

The regulatory circuit in which PhaR takes part was best studied in *Ralstonia eutropha* (17-19). In this bacterial species, PhaR binds to the promoter of its own gene, and to the promoter of *phaP*, which encodes a protein that binds to the surface of PHB granules named phasin (PhaP). Phasins contain amphipathic α-helices whereby these proteins may coat the hydrophobic granules during their growth, exposing a polar surface to the bulk cytoplasm (20, 21). It is believed that in this way the phasins may control the final size of PHB granules (22). In addition, PhaR also binds to the surface of PHB granules, although with less affinity than phasins (18). Thus, the model proposed for the regulation of PHB granules growth through PhaR/PhaP activities

suggests that while the granules are growing their surface area is enough to accommodate both PhaR and PhaP thus maintaining a low cytoplasmic concentration of free PhaR, which keeps the *phaR* and *phaP* promoters free. As the granules reach a critical volume, their surface area becomes limiting for PhaR and PhaP, which are continuously synthesized. At this point, PhaP displaces PhaR from the granules surface, raising the PhaR cytoplasmic concentration. The free PhaR binds *phaR* and *phaP* promoters, and the expression of both genes is inhibited, arresting PHB granules growth (18, 23). However, a recent study reported that the association constant of PhaR to its target DNA sequence in the *phaR* promoter is similar to that of an unspecific DNA sequence (24).

In *E. meliloti*, the symbiont of alfalfa, PhaP and PhaR (AniA) activities are necessary for PHB synthesis (16, 25). In addition, *phaR* (*aniA*) might play a more ample regulatory role of the carbon flow in *R. etli*. A *phaR*::Tn*5* mutant synthesized around 40% the PHB level of the wildtype and had significantly increased extracellular polysaccharide (EPS) levels, with extensive changes in its proteome (15). However, the regulatory circuit through which *phaR* may control EPS synthesis is unknown.

The genome of *B. diazoefficiens* USDA 110 harbors one copy of *phaR* (blr0227) which is located adjacent to PHB-related genes *phaA2* (bll0226) and *phaB2* (bll0225), but transcribed in the opposite direction (Fig. S1A). Meanwhile, at least four paralogs of *phaP* occur as isolated genes at locations elsewhere in the genome. The expression of these genes depends on the culture conditions. In particular, conditions permissive for PHB synthesis, such as microoxia (26) and growth in yeast-extract mannitol (YM) (14) increase the expression of *phaP1* and *phaP4*, the last being the paralog with highest expression in YM. PhaR and the four PhaP paralogs bind to PHB *in vitro* (14), being PhaP4 the phasin with highest affinity. Further, increasing concentration of PhaP4

Applied and Environmental Microbiology

triggered a competitive displacement of PhaR bound to PHB fine powder in suspension (14). These results suggested that PhaP4 could be the main phasin responsible for PhaP biological function in *B. diazoefficiens*. However, mutations of these genes were not obtained, and thus their implication in the regulation of PHB synthesis could not be directly established *in vivo*.

To better understand the regulation of PHB in *B. diazoefficiens* USDA 110, we constructed mutant strains in *phaR* and in two *phaP* genes and evaluated their roles in PHB and EPS synthesis, as well as in the symbiotic interaction with soybean plants.

MATERIALS AND METHODS

Bacterial strains and culture conditions. Strains and plasmids are summarized in Table S1. *B. diazoefficiens* was grown oxically or microoxically in Götz minimal medium with mannitol as the sole carbon source (27). For oxic growth, 50 ml cultures were grown in 250-ml Erlenmeyer flasks at 30°C with rotary shaking at 180 rpm in contact with the air. For microoxic growth, cells were inoculated into 500 ml-serum bottles containing 35 ml of Götz medium to an optical density at 500 nm (OD_{500}) of 0.03. The bottles were closed with rubber septa, and maintained at 30°C and 60 rpm in a microoxic condition by exchange of gas phase (0.5 % O_2, 99.5 % N_2) every 8 to 16 h until the desired growth state (26). Total biomass was estimated by OD_{500} and the number of viable bacteria by CFU counts on YM agar plates (28). Conjugation was performed in a modified peptone salts yeast extract medium (26). *Escherichia coli* was grown in Luria-Bertani (29). Antibiotics were added to the media at the following concentrations (μg ml^{-1}): streptomycin (Sm), 400 (*B. diazoefficiens*) or 100 (*E. coli*); spectinomycin (Sp), 200 (*B. diazoefficiens*) or 100 (*E. coli*); kanamycin (Km), 150 (*B. diazoefficiens*) or 25 (*E. coli*); ampicillin (Ap), 200 (*E. coli*); gentamicin (Gm), 100 (*B.*

128 *diazoefficiens*) or 10 (*E. coli*); tetracycline (Tc) 20 and 100 (*B. diazoefficiens* liquid and
129 solid cultures, respectively) or 10 (*E. coli*); and chloramphenicol (Cm), 20 (*B.*
130 *diazoefficiens*).
131
132 **Genetic techniques and DNA manipulation.** Cloning procedures, including DNA
133 isolation, restriction digestion, ligation, and transformation, were performed as
134 described (29). Tri- or biparental matings were performed with *E. coli* DH5α or S17-1
135 strains as described (3). Electroporation was performed with a Gene Pulser system (Bio-
136 Rad, Hercules, CA) at 1.5 V, 25 μF, and 200 Ω in a 0.1-cm-gap-width electroporation
137 cuvette.
138 Oligonucleotide primers were purchased from Life Technologies (Buenos Aires,
139 Argentina) or Sigma-Aldrich (Madrid, Spain). DNA amplification was performed by
140 PCR using Taq DNA polymerase (Life Technologies, Buenos Aires, Argentina) for
141 routine PCR or KAPA HiFi hot-start (HS) DNA polymerase (Kapabiosystems, Woburn,
142 MA) or Pfx (Life Technologies, Buenos Aires, Argentina) for the amplification of
143 blunt-ending amplicons and/or targets longer than 1,000 bp. DNA sequencing was
144 performed at Macrogen Corp. (Seoul, South Korea).
145 To construct the *B. diazoefficiens phaR* mutant, primers specific for the blr0227
146 locus tag were designed (Table S2). An internal 244 bp-PCR fragment was amplified
147 with primers Fw1 and Rv1 and cloned into pGEM-T easy creating pIQ35. This plasmid
148 was digested with EcoRI and ligated into pG18*mob*2, generating pIQ36, which was
149 conjugated into *B. diazoefficiens* LP 3004 by biparental mating using *E. coli* S17-1 as
150 the donor. Transconjugants were selected in Gm and Sm. We obtained two independent
151 clones by single homologous recombination of pIQ36 in the middle of the *phaR* coding
152 sequence, leading a predicted truncated polypeptide of 108 amino acids (58 % of the

153 full-length protein sequence). The results obtained regarding growth, PHB synthesis,
154 and extracellular polysaccharide production were similar with both clones, and therefore
155 we selected one of them that was designated LP 0227 (hereafter referred to as *phaR*
156 mutant; Fig. S1A).
157 For complementation, the complete sequence of *phaR* (amplified with primers
158 Fw1c/Rv1c) was integrated into a replicative vector. Briefly, a 1,245-bp target sequence
159 and its own putative promoter (inferred by BPROM program) were amplified from *B.*
160 *diazoefficiens* LP 3004 and cloned into the SmaI site of pBBR1-MCS-5 to create pIQ37.
161 Then, pIQ37 was digested with XbaI and PstI and the *phaR*-containing fragment was
162 inserted in the replicative broad-host-range promoter probe vector pCB303 (30),
163 generating plasmid pIQ38. The construction was confirmed by sequencing. The plasmid
164 was transferred into LP 0227 strain by biparental mating, selecting by growth on Tc and
165 Gm. The LP 0227 carrying pIQ38 turned blue in YM agar plates supplemented with X-
166 phosphate, thus confirming that the 1,245-bp fragment, cloned in the same orientation
167 of promoterless *phoA* gene in pIQ38, carried both the *phaR* promoter and the *phaR*
168 coding sequence.
169 To construct the *B. diazoefficiens* phasin mutants, primers specific for bll5155
170 (*phaP1*) or bll7395 (*phaP4*) locus tags were designed (Table S2). Fragments of *B.*
171 *diazoefficiens* USDA 110 genomic DNA were generated from both sides of the target
172 coding sequences. For both phasins, the strategy was similar. An upstream fragment of
173 249/253 bp and a downstream fragment of 235/222 bp were amplified using primers
174 Fw2/Rv2 or Fw3/Rv3 (fragments *phaP1-1* and *phaP4-1*, respectively) and Fw4/Rv4 or
175 Fw5/Rv5 (fragments *phaP1-2* and *phaP4-2*, respectively). The PCR fragments *phaP1-2*
176 and *phaP4-2* were cloned into SmaI site of pBBR1-MCS-4, creating pIQ39 and pIQ40.
177 These plasmids were then digested with EcoRV and the fragments *phaP1-1* and *phaP4-*

178 *1* were introduced, creating pIQ41 and pIQ42 respectively. These plasmids were
179 linealized with EcoRI. In parallel, pHP45ΩSmSp or pHP45ΩKm were EcoRI-digested,
180 and the resulting fragments ΩSm-Sp and ΩKm were cloned into pIQ41 and pIQ42,
181 creating pIQ43 and pIQ44, respectively. Finally, these two plasmids were digested with
182 XbaI and KpnI and the fragments of pIQ43 and pIQ44 were ligated into XbaI/KpnI-
183 digested pK18*mob* and pG18*mob*2, creating pIQ45 and pIQ46, respectively.
184 For *phaP1*, gene replacement was performed by introducing pIQ45 into *B.*
185 *diazoefficiens* USDA 110 by biparental mating, selecting by growth on Sm-Sp, and
186 screening for Km sensitivity. The resulting strain was designated LP 5155 (Δ*phaP1*);
187 this strain carries the Ω-Sm-Sp-interposon in place of the genomic DNA from base
188 5,711,611 to base 5,711,972, thus removing 301-bp from the 339-bp ORF bll5155 (Fig.
189 S1B). For *phaP4*, gene replacement was performed by introducing pIQ46 into *B.*
190 *diazoefficiens* USDA 110 by triparental mating using the pRK2013 helper plasmid,
191 selecting by growth on Km and Cm, and screening for Gm sensitivity. The resulting
192 strain was designated LP 7395 (Δ*phaP4*); this strain carries the Ω-Km-interposon in
193 place of the genomic DNA from base 8130454 to base 8130880, thus removing 426-bp
194 from the 435-bp ORF bll7395 (Fig. S1B). The double mutant LP 5173
195 (Δ*phaP1*/Δ*phaP4*) was constructed as described above, introducing pIQ45 in the
196 background of LP 7395.
197 All the mutations were confirmed by PCR using external primers (Table S2, Fig.
198 S1) as described previously (3), and by DNA sequencing.
199
200 **Bioinformatic characterization of PhaR and PhaP.** PhaR (Blr0227), PhaP1 (bll5155)
201 and PhaP4 (bll7395) were aligned with their putative homologs in *E. meliloti* 1021, *R.*
202 *etli* CFN42, *Azorhizobium caulinodans* ORS571 and *Rhizobium leguminosarum* bv

viciae 3841 using T-COFFEE (31). The secondary structure of PhaP1 and PhaP4 was predicted using Phyre2 alpha helix Prediction (http://www.sbg.bio.ic.ac.uk/phyre2) and PSIPRED v 3.3 Server (http://bioinf.cs.ucl.ac.uk/psipred/).

RNA isolation, cDNA synthesis, and quantitative reverse transcription PCR (qRT-PCR) analysis. *B. diazoefficiens* LP 3004 and *phaR* mutant cultures were grown microoxically as described above. The cultures were grown to mid-exponential phase at an OD_{500} of 0.25 to 0.33 (*phaR* mutant) or 0.50 to 0.62 (LP 3004) and were stopped by adding cool stop solution (equilibrated phenol and ethanol 1:9), collected by centrifugation at 4 °C and frozen at -80 °C as previously described (26, 32). This material was used for RNA isolation and cDNA synthesis as described elsewhere (33). Primers for qRT-PCR reactions were designed (Table S2) to have a melting temperature of 57°C to 62°C and to generate PCR products of 87 to 134 bp. Each PCR reaction contained 9.5 µl of iQ™ SYBR Green Supermix (Bio-Rad, Hercules, CA), 2 µM of individual primers and appropriate dilutions of different cDNAs in a total volume of 19 µl. Reactions were run in triplicate in a Bio-Rad iCycler. Melting curves were generated with Bio-Rad iQ5 software to verify the specificity of the amplification. Relative changes in gene expression (fold-changes) were calculated as described elsewhere (34). The fold-changes observed were considered significant when their absolute values were higher than 2.0. Expression of the primary sigma factor gene *sigA* was used as a reference for normalization.

Quantification and analysis of PHB and extracellular polysaccharides. For quantification of PHB, *B. diazoefficiens* cultures were centrifuged twice at 12,000 × *g* during 40 min. Then, the pellets were homogenized with sodium hypochlorite overnight

at room temperature, washed with double-distilled water, precipitated with 1:1 alcohol-acetone, and resuspended in chloroform. Then, PHB was determined as crotonic acid in H_2SO_4 (35). For analysis of composition, PHB was extracted from *B. diazoefficiens* lyophilized cells as described (36) and monomer composition was analyzed by gas chromatography (GC) after conversion of PHB to 3-hydroxybutyryl-methyl esters via acid methanolysis (36). Benzoate-methyl ester was used as internal standard.

To determine the PHB content of bacteroid cells, ten fresh mature nodules (70-90 mg) were washed, crushed and homogenized, suspended in 0.5 ml of double-distilled water, and centrifuged for 5 min at 5,000 × g (3). The supernatants were then processed for PHB determination as above.

Extracellular polysaccharides (EPS) include exopolysaccharide and capsular polysaccharide, which have the same sugar composition in *B. diazoefficiens* USDA 110 (37). Exopolysaccharides were precipitated from the culture supernatants as described (38) and capsular polysaccharides were released from bacterial cells and precipitated as described (37). Finally, the polysaccharides were hydrolyzed and the reducing sugars were quantified with anthrone as described (38).

Transmission electron microscopy (TEM). It was performed essentially as described (3, 38). Briefly, bacteria from liquid cultures or nodules (each one transversally cut in halves) were collected and fixed in 2% (vol/vol) glutaraldehyde. Next, the samples were dehydrated, infiltrated with epoxy resin, sectioned, and stained. Glutaraldehyde-fixed samples were placed in grids and viewed at 80 kV in a JEM1200 EX II transmission electron microscope (JEOL Ltd., Tokyo, Japan).

Applied and Environmental Microbiology

Some TEM micrographs of free-living cells were used to determine the diameter of PHB granules, using ImageJ software (version 1.49). The largest diameter of every individual granule was registered from each individual cell (n=132 to 411).

Plant experiments. DonMario 3810 soybean seeds, kindly provided by DonMario SA, Argentina, were surface sterilized, germinated, and cultivated in vermiculite pots as described (3). Stability of plasmid pIQ38 was verified by bacteroid isolation and CFU determination on plates containing Cm or Cm and Tc. Competition for nodulation was studied by inoculating LP 3004 and *phaR* mutant strains in a 1:1 proportion (as CFU ml^{-1}) to soybean plants as described (39). Nodule occupation was evaluated on the basis of the antibiotic resistance of the strains recovered from the nodules 21 days after inoculation. The statistical analysis was carried out with χ^2, considering 45% nodule occupation by each strain alone and 10% double occupation as the null hypothesis (38).

Plant growth parameters were assessed in 67-day-old plants. Shoots from each plant were cut and dried in an oven at 60°C to constant weight, and the materials from each plant were weighed individually. The statistical analysis was performed by one-way analysis of variance (ANOVA), with $\alpha < 0.05$. All results shown are representative of duplicate experiments.

RESULTS

***B. diazoefficiens* produces PHB homopolymer.** The polyhydroxyalkanoates extracted from lyophilized cells of *B. diazoefficiens* USDA 110 (wildtype), LP 3004 (wildtype, spontaneous Sm-resistant derivative from USDA 110) and *phaR* mutant strains from exponential (7 days) and late stationary-phase (25 days) cultures in oxic conditions (Fig. 1A) were characterized for composition of their monomer units by GC analysis. GC-

chromatograms from both culture ages were similar, and those corresponding to stationary phase are shown in Fig. S2. As observed, polyhydroxyalkanoates of the three strains tested possess only 3-hydroxybutyrate units. This finding allowed us to quantify the polyhydroxyalkanoate contents by the detection of crotonic acid at 235 nm, because this specific analysis method applies only for Poly(3HB) (35).

PHB and EPS synthesis are controlled by *phaR* under oxygen-limiting conditions. We measured total biomass (as OD_{500}) daily in oxic cultures for 25 days in the wild-type, *phaR* mutant and mutant-complemented strains (Fig. 1A). There were no differences in exponential growth rates but the stationary phase was reached earlier in the *phaR* mutant, resulting in reduced biomass with respect to the wildtype and mutant-complemented strains. Next, we measured PHB levels at 7 (logarithmic), 13 (early-stationary), 17 (middle-stationary) and 25 (late-stationary) days of growth. The production of PHB at 7 days of growth was higher in the *phaR* mutant than in the wildtype, but later there was a strong increase in PHB production in the wildtype at early- middle- and late-stationary phase that was not observed in the *phaR* mutant (Fig. S3A). At late-stationary phase, the mutant-complemented strain accumulated more PHB than the mutant, but only half the wildtype PHB levels (Fig. 1B). In addition, we measured EPS contents at the same growth states. Whilst there were no differences between strains at logarithmic and early- and middle-stationary phase (data not shown), at late-stationary phase the *phaR* mutant produced about 4-fold more EPS in comparison to that determined in wildtype and *phaR*-complemented strains (Fig. 1C), which was also reflected macroscopically in the high mucoidy of *phaR* mutant cell pellets after centrifugation (Fig. S3B). TEM of 25 day-old cells (Fig. 1D-F) showed that, while the *phaR* mutant cells were devoid of PHB granules, the wildtype and the *phaR*

Applied and Environmental Microbiology

mutant-complemented strains had PHB granules (in the complemented strain, most cells had a single large granule).

By contrast, in microoxic cultures the growth rate and total biomass of the *phaR* mutant were smaller than the wildtype or the mutant-complemented strain from the beginning of the culture (Fig. 1G). Likewise, PHB production was affected in the mutant at early-stationary phase (11 days of growth), being restored in the mutant-complemented strain (Fig. 1B). These results, in agreement with previous investigations (3, 27, 40) indicated that the microoxia and the stationary phase of oxic cultures were permissive conditions for PHB synthesis, while exponential phase of oxic cultures was non-permissive. In addition, the oxygen-limiting bacteroid state inside root nodules is also a permissive condition (3). Our results indicate that the activity of PhaR on PHB production is mainly exerted under these permissive conditions.

PhaR exerts a negative control on PHB-related genes and *fixK*$_2$ expression. The permissive conditions indicated above have in common that they involve oxygen limitation. Because oxic cultures of the *phaR* mutant at late-stationary phase produce too much EPS that interferes with RNA extraction, we evaluated the role of PhaR as a transcriptional regulator in mid-exponential phase microoxic cultures. We compared the levels of certain transcripts in the *phaR* mutant and the wildtype by qRT-PCR, as summarized in Fig. 2. The levels of most of the transcripts were lower in the wildtype indicating that *phaR* is a repressor, in agreement with previous reports (41). However, the mutation of *phaR* had no effect on its own transcription, which is in line with the low association constant of PhaR to its target DNA sequence at the *phaR* promoter region described in *R. eutropha* H16 (24).

Phasin genes are known as direct targets of *phaR*. In *B. diazoefficiens* there are at least four paralogs encoding phasins, of which *phaP1* and *phaP4* have the highest expression level (14, 26) and PhaP4 the highest affinity for PHB *in vitro* (14). Therefore, we assessed the expression of these two phasin genes and found that transcription of *phaP1* and *phaP4* were strongly derepressed in the *phaR* mutant, *phaP1* being the most affected.

In addition, we evaluated the transcript levels of genes encoding enzymes of the PHB biosynthetic pathway. Particularly, we assessed the 3-ketoacyl-CoA thiolase paralogs *phaA1* and *phaA2*, and the PHB synthase paralogs *phaC1*, *phaC2*, and *phaC3*. Of these three PHB synthase-coding genes, only *phaC1* is required (3). In turn, a deletion of *phaC2* causes significant increases in PHB synthesis, while PhaC3 seems active only in a *phaC2*-mutant background (3). We observed that *phaC2* was significantly (13-fold) upregulated and transcription of *phaC1* was increased 5-fold while transcription of *phaC3* was not affected in the *phaR* mutant. The most upregulated in the mutant was *phaC2*, and interestingly, this gene was previously reported as positively controlled by the global regulator $fixK_2$ (26). In the same line as the Δ*phaC2*, a Δ$fixK_2$ strain also accumulated more PHB than the wildtype in stationary phase (Fig. S4). Therefore, we also measured the amounts of $fixK_2$ transcripts, and found that, as with the other genes, mutation of *phaR* resulted in ≈6-fold upregulation of $fixK_2$ transcription.

Phasin mutants showed an altered pattern of PHB granule size and accumulation. The secondary-structure prediction analysis of PhaP1 and PhaP4 indicated a high prevalence of alpha helix structure (91 and 86% respectively, data not shown), compatible with known phasins. Moreover, growth kinetics of the deletion mutants

Δ*phaP1*, Δ*phaP4*, and Δ*phaP1*/Δ*phaP4* was similar to the wildtype, indicating that none of the phasin genes is essential for growth in *B. diazoefficiens*. In addition, PHB accumulation in the single mutants was similar to the wildtype at middle-stationary phase, but the Δ*phaP1*/Δ*phaP4* strain accumulated ≈3-times more PHB (Fig. 3A). However, although Δ*phaP4* produced PHB granules that did not differ significantly from the wildtype (0.420 µm ± 0.134 and 0.521 µm ± 0.145 in diameter, respectively), Δ*phaP1* produced smaller granules (0.304 µm ± 0.115), but in more quantity than the wildtype (Fig. S5). In addition, Δ*phaP1*/Δ*phaP4* cells had large PHB granules (0.774 µm ± 0.140, Fig S5) that occupied a considerable portion of the cytoplasm (Fig. 3E), similarly to a *phaP1* mutant in *R. eutropha* (23, 42). Thus, an influence of PhaP1 on granule surface/volume ratio as well as an interaction between PhaP1 and PhaP4 for controlling the growth of the granules may be appreciated.

The *phaR* mutant has a better symbiotic performance than the wildtype. Previous reports on nodulation of *phaR* mutants are contradictory. On the one hand, the *E. meliloti phaR* mutant formed many pseudonodules in alfalfa negatively altered in N_2 fixation (16); on the other hand, the *R. etli phaR* mutant produced macroscopically normal nodules in common bean, without significant differences in nitrogenase activity with respect to the wildtype (15). However, nodulation differs among these host plants, because alfalfa produces indeterminate nodules without PHB, while common bean produces determinate nodules, which has typical PHB granules in the bacteroidal cytoplasm. Since soybean produces determinate nodules, we wanted to know if our *phaR* mutant behaves similarly as *R. etli* for its symbiotic interaction with soybean roots.

As in *R. etli*-common bean, soybean plants inoculated with the *B. diazoefficiens phaR* mutant produced morphologically normal nodules. However, when nodules from

67 day-old plants were observed by TEM, it became evident that they were completely devoid of PHB granules (Fig. 4B). When this mutant was complemented with the wildtype *phaR* gene in *trans*, the production of PHB granules in soybean nodules was restored, indicating that the mutation in *phaR* was responsible for the lack of PHB granules production in the mutant bacteroids (Fig. 4C), as observed above in free-living conditions. Furthermore, the analytic determination of PHB levels from crushed nodules corroborated these observations (Fig. 4D). It is possible that the low PHB levels detected in nodules infected by the *phaR* strain (0.03 µg.mg nodule fresh weight^{-1}) correspond to PHB granules from bacteria (not bacteroids) that remained into the infection threads.

Competition for nodulation was evaluated by inoculating soybean plants with 1:1 mixtures of wildtype and *phaR* mutant strains, each one at a concentration in the order of 10^5 cfu ml^{-1}. Because late-stationary cultures are poor competitors (40), and we wanted to compare permissive and non-permissive conditions, we prepared the inocula from oxic cultures either in exponential phase (non-permissive) or in middle-stationary phase (permissive). As a result, we observed in two independent experiments that in non-permissive conditions the competitiveness of both strains was similar, while under permissive conditions the *phaR* mutant was more competitive than the wildtype, occupying 74% of the nodules (Fig. 4E).

Despite differences in competitiveness, there were no differences in the number of nodules produced by the wildtype and the *phaR* mutant (Fig. 4F). However, the shoot dry weight of 67 day-old plants cultured in nutrient solution without combined nitrogen was significantly higher in the plants inoculated with the *phaR* mutant (Fig. 4F). This result suggests that each nodule occupied by the *phaR* mutant was more active than those occupied by the wildtype.

DISCUSSION

As observed in other bacterial species, *phaR* was necessary for the production of PHB in microoxic and old oxic cultures of *B. diazoefficiens*. In addition, mutation of *phaR* impaired biomass accumulation of old oxic cultures in stationary phase, and compromised the growth of microoxic cultures at all growth phases. These results indicate that PhaR exerts its activity under conditions of oxygen limitation, in which accumulation of substrates for the PHB synthesis, like reducing power and acetyl-CoA, may take place. In addition, lack of PHB granules in our *phaR* mutant was accompanied by higher production of EPS, a correlation previously observed in *E. meliloti* (16), *R. etli* (15) and N-limited *B. diazoefficiens* wildtype cultures (27, 40). However, a plausible explanation on how *phaR* also controls the EPS synthesis is lacking. Interestingly, PhaR also appeared as repressor of $fixK_2$, a global regulator which activates the expression of more than two hundred genes needed for life under low oxygen tension, including essential operons such as *fixNOQP* and *fixGHIS* (26, 43, 44). Because the expression of *phaR* is not affected in a $\Delta fixK_2$ strain grown under oxygen-limiting conditions (26), it seems that *phaR* is at the highest hierarchy of this regulatory circuit. Therefore, the regulation scope of PhaR may be wider than previously thought. In Fig. 5 we propose an extended model for the regulation of PHB synthesis including the findings obtained in this work.

At least three pathways may explain the initiation of PHB synthesis in *R. eutropha* (6) but it is unknown which of them is functional in *B. diazoefficiens*. Our results indicate that after initiation under permissive conditions, PHB synthesis would be catalyzed by basal levels of 3-ketoacyl-CoA thiolase, acetoacetyl-CoA reductase, and PHB synthase using microoxically accumulated reducing power and acetyl-CoA as

425 substrates. At this point, *phaR* may be expressed, but since the surface/volume ratio of
426 the PHB granule is large, most of the PhaR produced should bind the PHB granule
427 surface, leaving the *phaC1*, *phaC2*, *phaP1*, *phaP4*, and *fixK*$_2$ promoters free. FixK$_2$
428 stimulates the expression of *phaC2*, which encodes an inactive PHB synthase subunit
429 that, by mass action, may impair the formation of PhaC1/PhaC1 fully active
430 homodimers, while increasing the concentration of PhaC1/PhaC2 less active
431 heterodimers and PhaC2/PhaC2 inactive homodimers (3, 14, 17, 45). Thus, the
432 juxtaposition of *phaR* and *fixK*$_2$ on *phaC2* regulation might allow a fine-tuning of the
433 whole PHB synthase activity at the stage of PHB granules growth. Interestingly, *fixK*$_2$
434 and *phaC2* are also induced under conditions of oxidative burst, where an increase in
435 EPS production was also observed (46). Therefore, we can speculate that PHB synthesis
436 might be diminished under oxidative damage, perhaps by downregulation of *phaR*. In
437 addition to PhaC2, the phasins PhaP1 and PhaP4 may play an important role in
438 controlling the size of PHB granules. Although PhaP4 seems to be the main protein
439 covering PHB granules (14), only the double mutant Δ*phaP1*/Δ*phaP4* synthesized more
440 PHB than the wildtype. Moreover, when both phasins were missing, the PHB granule
441 surface/volume ratio decreased and the bacteria possessed only one large granule per
442 cell, resembling other bacterial phasin mutants (23, 47). Hence, in *B diazoefficiens*, the
443 combined function of PhaP1 and PhaP4 could prevent PHB granules coalescence, as
444 reported in *R. eutropha* (42). This combined function suggests that in *B. diazoefficiens*
445 phasins could form trimers and/or tetramers as in other PHB-producing bacteria (48-50)
446 as homo- and/or hetero-oligomers. In this way, the relative concentrations of PhaC1 and
447 PhaC2 may modulate PHB synthase activity while the production of PhaP1 and PhaP4
448 may control the number and size of PHB granules. As the granules reach their final
449 sizes, PhaR would be released from their surface exerting its inhibitory effect towards

all these PHB synthesis proteins. According to this model, the higher accumulation of PHB in the Δ*phaP1*/Δ*phaP4* strain might be explained by a high PhaR sequestration at the PhaP1- and PhaP4-devoid PHB granule in formation, which might promote higher expression of PHB biosynthetic genes before the PhaC2/PhaC1 ratio reaches its critical value to inhibit PHB synthase activity and free PhaR begins to increase. The presence of one large granule per cell indicates that each granule grows rapidly within a single cell cycle.

In addition to its action upon *phaC2* expression, $FixK_2$ was reported to stimulate the expression of bll3998 (a succinate-semialdehyde dehydrogenase) and blr4655 (a phospho*enol*pyruvate synthase) (26). The succinate-semialdehyde dehydrogenase, which catalyzes the oxidation of succinate-semialdehyde to succinate using $NADP^+$ as electron acceptor, was characterized in a *sucA* mutant of *B. diazoefficiens* as part of a bypass of the TCA cycle (51). The phospho*enol*pyruvate synthase is a key enzyme of gluconeogenesis and may participate in secretion of excess carbon as EPS. Thus, induction of $fixK_2$ under permissive conditions might increase the provision of NADPH to PHB synthesis while this pathway is active, or might contribute to the switch of the carbon flow to gluconeogenesis when PHB synthesis is arrested by PhaP coverage of PHB granules and PhaC2 relative increased participation in the PHB synthase dimers (Fig. 5). This hypothesis might explain the inhibition of PHB synthesis and increase in EPS content observed with the *phaR* mutants in *E. meliloti* (16), *R. etli* (15), and in this work. If *phaR* is knocked out, the expression of *phaC2* and *phaP* become uncontrolled and therefore, the accumulation of their products would lead to rapid inhibition of PHB synthesis and granule growth. In parallel, $fixK_2$ expression is induced, which would stimulate the expression of the succinate-semialdehyde dehydrogenase and the phospho*enol*pyruvate synthase. The precursors provided by the first enzyme could not

Applied and Environmental Microbiology

be used for PHB synthesis because it is arrested, and as gluconeogenesis may be stimulated by the second enzyme, those precursors could be channeled to synthesis and secretion of EPS.

In symbiosis, the phenotype observed here also indicated that *phaR* plays a pleiotropic function. Previously we observed that lack of PHB in *B. diazoefficiens* Δ*phaC1* strains led to decreased competitiveness for nodulation, but had no effects on dry matter accumulation in plants cultured without combined nitrogen, indicating that N_2 fixation was not affected (3). By contrast, here we observed an increase in competitiveness for nodulation of the *phaR* mutant grown under permissive conditions for PHB synthesis, as well as an increase in dry matter accumulation in plants inoculated with the *phaR* mutant and cultured under N_2-fixing conditions. Because the *phaR* mutant bacteroids also had no PHB granules in their cytoplasm, the comparison of the results obtained with *phaC1* and *phaR* mutants indicate that the symbiotic phenotypes of the *phaR* mutants are not related only to PHB depletion. It is possible that in Δ*phaC1*, the cytoplasmic levels of PhaR are high because of the absence of PHB granules, and in this way, the expression of the $fixK_2$ regulon, which includes the regulators $rpoN_1$, $fixK_1$ and *nnrR* (26), might be repressed by PhaR. By contrast, overexpression of $fixK_2$ in the *phaR* mutants would favor the expression of these genes and in particular, it might lead to higher N_2 fixation via the expression of the alternative sigma factor $RpoN_1$ (26). Nevertheless, we should not rule out an active role of EPS in the symbiotic performance of *phaR* mutant due to its higher production in this strain.

Thus, the present results confirm the role of *phaR* as a global regulator both in free-living and symbiotic states, suggesting that this role may be exerted at two levels: directly on PHB synthesis and indirectly on other pathways through regulation of the transcription factor $fixK_2$.

ACKNOWLEDGMENTS

This work was supported by ANPCyT, CONICET (Argentina), MINECO-Spain (ERDF-cofinanced grant AGL2011-23383) and the Deutsche Forschungsgemeinschaft (Germany) (Je 152/17-1). The authors are grateful to Paula Giménez, Silvana Tongiani, Abel Bortolameotti, and Jesús Chacón for technical assistance. We also thank Susana Jurado and Roxana Peralta (Servicio Central de Microscopía, Facultad de Ciencias Veterinarias, UNLP, La Plata, Argentina) for excellent assistance with electron microscopy.

REFERENCES

1. Delamuta JR, Ribeiro RA, Ormeño-Orrillo E, Melo IS, Martínez-Romero E, Hungria M. 2013. Polyphasic evidence supporting the reclassification of *Bradyrhizobium japonicum* group Ia strains as *Bradyrhizobium diazoefficiens* sp. nov. Int J Syst Evol Microbiol **63:**3342-3351. doi: 10.1099/ijs.0.049130-0.

2. Madison LL, Huisman GW. 1999. Metabolic engineering of poly (3-hydroxyalkanoates): from DNA to plastic. Microbiol Mol Biol Rev **63:**21-53.

3. Quelas JI, Mongiardini EJ, Pérez Giménez J, Parisi G, Lodeiro AR. 2013. Analysis of two polyhydroxyalkanoate (PHA) synthases in *Bradyrhizobium japonicum* USDA 110. J Bacteriol **195:**3145-3155. doi: 10.1128/JB.02203-12.

4. Khanna S, Srivastava AK. 2005. Recent advances in microbial polyhydroxyalkanoates. Process Biochem **40:**607-619.

523 **5. Urtuvia V, Villegas P, González M, Seeger M.** 2014. Bacterial production of the
524 biodegradable plastics polyhydroxybutyrates. Int J Biol Macromol **70:**208-213. doi:
525 10.1016/j.ijbiomac.2014.06.001.

526 **6. Jendrossek D, Pfeiffer D.** 2014. New insights in the formation of
527 polyhydroxyalkanoate granules (carbonosomes) and novel functions of poly(3-
528 hydroxybutyrate). Environ Microbiol **16:**2357-2373. doi: 10.1111/1462-2920.12356.

529 **7. Ratcliff WC, Kadam SV, Denison RF.** 2008. Poly-3-hydroxybutyrate (PHB)
530 supports survival and reproduction in starving rhizobia. FEMS Microbiol Ecol **65:**391-
531 399. doi: 10.1111/j.1574-6941.2008.00544.x.

532 **8. Taidi B, Mansfield D, Anderson AJ.** 1995. Turnover of poly(3-hydroxybutyrate)
533 (PHB) and its influence on the molecular mass of the polymer accumulated by
534 *Alcaligenes eutrophus* during batch culture. FEMS Microbiol Lett **129:**201-206.

535 **9. Pötter M, Steinbüchel A.** 2005. Poly(3-hydroxybutyrate) granule-associated
536 proteins: impacts on poly(3-hydroxybutyrate) synthesis and degradation.
537 Biomacromolecules **6:**552-560.

538 **10. Uchino K, Saito T, Jendrossek D.** 2007. Poly(3-hydroxybutyrate) (PHB)
539 depolymerase PhaZ1 is involved in mobilization of accumulated PHB in *Ralstonia*
540 *eutropha* H16. Appl Environ Microbiol **74:**1058-1063.

541 **11. Eggers J, Steinbüchel A.** 2013 Poly(3-hydroxybutyrate) degradation in *Ralstonia*
542 *eutropha* H16 is mediated stereoselectively to (S)-3-hydroxybutyryl coenzyme A (CoA)
543 via crotonyl-CoA. J Bacteriol **195:**3213-3223. doi: 10.1128/JB.00358-13.

544 **12. Sznajder A, Pfeiffer D, Jendrossek D.** 2015. Comparative proteome analysis
545 reveals four novel polyhydroxybutyrate (PHB) granule-associated proteins in *Ralstonia*
546 *eutropha* H16. Appl Environ Microbiol **81:**1847-1858. doi: 10.1128/AEM.03791-14.

547 **13. Aneja P, Dai M, Lacorre DA, Pillon B, Charles TC.** 2004. Heterologous
548 complementation of the exopolysaccharide synthesis and carbon utilization phenotypes
549 of *Sinorhizobium meliloti* Rm1021 polyhydroxyalkanoate synthesis mutants. FEMS
550 Microbiol Lett **239:**277-283.

551 **14. Yoshida K, Takemoto Y, Sotsuka T, Tanaka K, Takenaka S.** 2013. PhaP phasins
552 play a principal role in poly-β-hydroxybutyrate accumulation in free-living
553 *Bradyrhizobium japonicum*. BMC Microbiol **13:**290. doi: 10.1186/1471-2180-13-290.

554 **15. Encarnación S, Vargas MC, Dunn MF, Dávalos A, Mendoza G, Mora Y, Mora**
555 **J.** 2002. AniA regulates reserve polymer accumulation and global protein expression in
556 *Rhizobium etli*. J Bacteriol **184:**2287-2295.

557 **16. Povolo S, Casella S.** 2000. A critical role for *aniA* in energy-carbon flux and
558 symbiotic nitrogen fixation in *Sinorhizobium meliloti*. Arch Microbiol **174:**42-49.

559 **17. Seo MC, Shin HD, Lee YH.** 2004. Transcription level of granule-associated *phaP*
560 and *phaR* genes and granular morphogenesis of poly-beta-hydroxyalkanoate granules in
561 *Ralstonia eutropha*. Biotechnol Lett **26:**617-622.

562 **18. Pötter M, Madkour MH, Mayer F, Steinbüchel A.** 2002. Regulation of phasin
563 expression and polyhydroxyalkanoate (PHA) granule formation in *Ralstonia eutropha*
564 H16. Microbiology **148:**2413-2426.

565 **19. York GM, Stubbe J, Sinskey, AJ.** 2002. The *Ralstonia eutropha* PhaR protein
566 couples synthesis of the PhaP phasin to the presence of polyhydroxybutyrate in cells
567 and promotes polyhydroxybutyrate production. J Bacteriol **184:**59-66.

568 **20. Mezzina MP, Wetzler DE, Catone MV, Bucci H, Di Paola M, Pettinari MJ.**
569 2014. A phasin with many faces: structural insights on PhaP from *Azotobacter* sp. FA8.
570 PLoS One **9:**e103012. doi: 10.1371/journal.pone.0103012.

571 **21. Hauf W, Watzer B, Roos N, Klotz A, Forchhammer K.** 2015. Photoautotrophic
572 polyhydroxybutyrate granule formation is regulated by cyanobacterial phasin PhaP in
573 *Synechocystis* sp. strain PCC 6803. Appl Environ Microbiol **81:**4411-4422. doi:
574 10.1128/AEM.00604-15.

575 **22. Kuchta K, Chi L, Fuchs H, Pötter M, Steinbüchel A.** 2007. Studies on the
576 influence of phasins on accumulation and degradation of PHB and nanostructure of
577 PHB granules in *Ralstonia eutropha* H16. Biomacromolecules **8:**657-662.

578 **23. Pötter M, Müller H, Steinbüchel A.** 2005. Influence of homologous phasins
579 (PhaP) on PHB accumulation and regulation of their expression by the transcriptional
580 repressor PhaR in *Ralstonia eutropha* H16. Microbiology **151:**825-833.

581 **24. Yamada M, Takahashi S, Okahata Y, Doi Y, Numata K.** 2013. Monitoring and
582 kinetic analysis of the molecular interactions by which a repressor protein, PhaR, binds
583 to target DNAs and poly[(R)-3-hydroxybutyrate]. AMB Express **3:**6. doi:
584 10.1186/2191-0855-3-6.

585 **25. Wang C, Sheng X, Equi RC, Trainer MA, Charles TC, Sobral BW.** 2007.
586 Influence of the poly-3-hydroxybutyrate (PHB) granule-associated proteins (PhaP1 and

587 PhaP2) on PHB accumulation and symbiotic nitrogen fixation in *Sinorhizobium meliloti*
588 Rm1021. J Bacteriol **189:**9050-9056.

589 **26. Mesa S, Hauser F, Friberg M, Malaguti E, Fischer H-M, Hennecke H.** 2008.
590 Comprehensive assessment of the regulons controlled by the FixLJ-$FixK_2$-$FixK_1$
591 cascade in *Bradyrhizobium japonicum*. J Bacteriol **190:**6568-6579. doi:
592 10.1128/JB.00748-08.

593 **27. Quelas JI, López-García SL, Casabuono A, Althabegoiti MJ, Mongiardini EJ,**
594 **Pérez-Giménez J, Couto A, Lodeiro AR.** 2006. Effects of N-starvation and C-source
595 on exopolysaccharide production and composition in *Bradyrhizobium japonicum*. Arch
596 Microbiol **186:**119-128.

597 **28. Vincent JM.** 1970. A manual for the practical study of the root nodule bacteria. IBP
598 handbook No. 15. Blackwell Scientific Publications. Oxford, UK.

599 **29. Sambrook J, Russell D.** 2001. Molecular cloning: a laboratory manual. Cold
600 Spring Harbor Laboratory Press, Cold Spring Harbor, NY.

601 **30. Schneider K, Beck CF.** 1987. New expression vectors for identifying and testing
602 signal structures for initiation and termination of transcription. Methods Enzymol
603 **153:**452-461.

604 **31. Notredame C, Higgins DG Heringa J.** 2000. T-Coffee: a novel method for fast
605 and accurate multiple sequence alignment. J Mol Biol **302:**205-217.

606 **32. Hauser F, Pessi G, Friberg M, Weber C, Rusca N, Lindemann A, Fischer H-M,**
607 **Hennecke H.** 2007. Dissection of the *Bradyrhizobium japonicum* NifA+σ^{54} regulon,

608 and identification of a ferredoxin gene (*fdxN*) for symbiotic nitrogen fixation. Mol
609 Genet Genomics **278:**255-271.

610 **33. Torres MJ, Argandoña M, Vargas C, Bedmar EJ, Fischer H-M, Mesa S,**
611 **Delgado MJ.** 2014. The global response regulator RegR controls expression of
612 denitrification genes in *Bradyrhizobium japonicum*. PLoS One **9:**e99011. doi:
613 10.1371/journal.pone.0099011.

614 **34. Pfaffl MW.** 2001. A new mathematical model for relative quantification in real-
615 time RT-PCR. Nucleic Acids Res **1:**29-45.

616 **35. Law JH, Slepecky RA.** 1961. Assay of poly-hydroxybutyric acid. J Bacteriol
617 **82:**33-36.

618 **36. Brandl H, Gross RA, Lenz RW, Fuller RC.** 1988. *Pseudomonas oleovorans* as a
619 source of poly(beta-hydroxyalkanoates) for potential applications as biodegradable
620 polyesters. Appl Environ Microbiol **54:**1977-1982.

621 **37. Mort AJ, Bauer WD.** 1980. Composition of the capsular and extracellular
622 polysaccharides of *Rhizobium japonicum*. Changes with culture age and correlations
623 with binding of soybean seed lectin to the bacteria. Plant Physiol **66:**158-163.

624 **38. Quelas JI, Mongiardini EJ, Casabuono A, López-García SL, Althabegoiti MJ,**
625 **Covelli JM, Pérez-Giménez J, Couto A, Lodeiro AR.** 2010. Lack of galactose or
626 galacturonic acid in *Bradyrhizobium japonicum* USDA 110 exopolysaccharide leads to
627 different symbiotic responses in soybean. Mol Plant-Microbe Interact **23:**1592-1604.
628 doi: 10.1094/MPMI-05-10-0122.

629 **39. Althabegoiti MJ, Covelli JM, Pérez-Giménez J, Quelas JI, Mongiardini EJ,**
630 **López MF, López-García SL, Lodeiro AR.** 2011. Analysis of the role of the two
631 flagella of *Bradyrhizobium japonicum* in competition for nodulation of soybean. FEMS
632 Microbiol Lett **319:**133-139. doi: 10.1111/j.1574-6968.2011.02280.x.

633 **40. López-García S, Vázquez TEE, Favelukes G, Lodeiro A.** 2001. Improved
634 soybean root association of N-starved *Bradyrhizobium japonicum*. J Bacteriol
635 **183:**7241-7252.

636 **41. Maehara A, Taguchi S, Nishiyama T, Yamane T, Doi Y.** 2002. A repressor
637 protein, PhaR, regulates polyhydroxyalkanoate (PHA) synthesis via its direct interaction
638 with PHA. J Bacteriol **184:**3992-4002.

639 **42. Wieczorek R, Pries A, Steinbüchel A, Mayer F.** 1995. Analysis of a 24-kilodalton
640 protein associated with the polyhydroxyalkanoic acid granules in *Alcaligenes eutrophus*.
641 J Bacteriol **177:**2425-2435.

642 **43. Mesa S, Reutimann L, Fischer H-M, Hennecke H.** 2009. Posttranslational control
643 of transcription factor $FixK_2$, a key regulator for the *Bradyrhizobium japonicum*-
644 soybean symbiosis. Proc Natl Acad Sci U S A **106:**21860-21865. doi:
645 10.1073/pnas.0908097106.

646 **44. Nellen-Anthamatten D, Rossi P, Preisig O, Kullik I, Babst M, Fischer H-M,**
647 **Hennecke H.** 1998. *Bradyrhizobium japonicum* $FixK_2$, a crucial distributor in the
648 FixLJ-dependent regulatory cascade for control of genes inducible by low oxygen levels
649 J Bacteriol **180:**5251-5255.

650 **45. Jendrossek D.** 2009. Polyhydroxyalkanoate granules are complex subcellular
651 organelles (carbonosomes). J Bacteriol **191:**3195-3202. doi: 10.1128/JB.01723-08.

652 **46. Donati AJ, Jeon JM, Sangurdekar D, So JS, Chang WS.** 2011. Genome-wide
653 transcriptional and physiological responses of *Bradyrhizobium japonicum* to paraquat-
654 mediated oxidative stress. Appl Environ Microbiol **77:**3633-3643. doi:
655 10.1128/AEM.00047-11.

656 **47. Cai S, Cai L, Liu H, Liu X, Han J, Zhou J, Xiang H.** 2012. Identification of the
657 haloarchaeal phasin (PhaP) that functions in polyhydroxyalkanoate accumulation and
658 granule formation in *Haloferax mediterranei*. Appl Environ Microbiol **78:**1946-1952.
659 doi: 10.1128/AEM.07114-11.

660 **48. Neumann L, Spinozzi F, Sinibaldi R, Rustichelli F, Pötter M, Steinbüchel A.**
661 2008. Binding of the major phasin, PhaP1, from *Ralstonia eutropha* H16 to poly(3-
662 hydroxybutyrate) granules. J Bacteriol **190:**2911-2919. doi: 10.1128/JB.01486-07.

663 **49. Zhao M, Li Z, Zheng W, Lou Z, Chen GQ.** 2006. Crystallization and initial X-ray
664 analysis of polyhydroxyalkanoate granule-associated protein from *Aeromonas*
665 *hydrophila*. Acta Crystallogr Sect F Struct Biol Cryst Commun **62:**814-819.

666 **50. Pfeiffer D, Jendrossek D.** 2011. Interaction between poly(3-hydroxybutyrate)
667 granule-associated proteins as revealed by two-hybrid analysis and identification of a
668 new phasin in *Ralstonia eutropha* H16. Microbiology **157:**2795-2807. doi:
669 10.1099/mic.0.051508-0.

670 **51. Green LS, Li Y, Emerich DW, Bergersen FJ, Day DA.** 2000. Catabolism of α-
671 ketoglutarate by a *sucA* mutant of *Bradyrhizobium japonicum*: evidence for an
672 alternative tricarboxylic acid cycle. J Bacteriol **182:**2838-2844.

673

674 **LEGENDS TO FIGURES.**

675 **FIG 1** Physiological characterization of the *phaR* mutant in oxic or microoxic
676 conditions. (**A-F**) Oxic conditions, with rotary shaking at 180 rpm in contact with the
677 air. (**A**) Growth kinetics. (**B**) PHB extracted from 25 day-old cells. (**C**) EPS obtained
678 from 25 day-old cultures. (**D-F**) Transmission electron micrographs of cells from 25
679 day-old cultures showing bright PHB granules (scale bar: 0.2 µm). (**G-H**) Microoxic
680 conditions, with rotary shaking at 60 rpm in contact with an atmosphere of 0.5 % O_2
681 and 99.5 % N_2. **G**: Growth kinetics. (**H**) PHB extracted from 11 day-old cells. In all
682 cases, quantitative results are average ± SME from four independent cultures. When
683 error bars are not visible, they are smaller than the symbol.

684 **FIG 2** Differential expression of selected genes among the wildtype and the *phaR*
685 mutant, evaluated by qRT-PCR in cells grown microoxically. Fold-change refers to the
686 relative expression in the mutant to the wildtype. An absolute value of fold-change ≥ 2
687 (line of reference) was considered statistically significant. Results are average from
688 three runs ± SME.

689 **FIG 3** PHB accumulation in the wildtype and three Δ*phaP* mutant derivatives,
690 evaluated at 17 days in oxic conditions. (**A**) PHB extracted from cells, expressed as
691 average from four independent determinations ± SME. (**B-E**) Transmission electron
692 micrographs of the wildtype (**B**), Δ*phaP*1 (**C**), Δ*phaP*4 (**D**), and Δ*phaP*1/Δ*phaP*4 (**E**).
693 Note the PHB granules as bright spots inside the cytoplasm. Scale bars: 0.5 µm.

694 **FIG 4** Effects of *phaR* on the symbiotic interaction with soybean plants. (**A-C**)
695 Transmission electron micrographs of ultrathin cuts of 67-day-old soybean nodules
696 showing bacteroids. (**A**) wildtype; (**B**) *phaR* mutant; (**C**) *phaR* mutant-complemented.

Note the PHB granules as bright spots in (**A**) and (**C**). Scale bars: 0.5 µm. (**D**) Average PHB content (± SME) from soybean nodules obtained from ten 67-day-old plants inoculated with the indicated strains. (**E**) Percentage of nodules occupied by the wildtype (black bars) or the *phaR* mutant (white bars) inoculated in 1:1 mixtures on 10 soybean plants. Inoculants were prepared with cultures harvested at the physiological states indicated. (**F**) Shoot dry weight and nodulation of 10 soybean plants inoculated with the wild-type (black bars) or the *phaR* mutant (white bars) after 67 days of growth. Values shown are after subtracting the uninoculated control (shoot dry weight: 0.658 ± 0.09 g plant^{-1}; nodules: 0). Asterisks in (**E-F**) indicate statistically significant differences ($\alpha < 0.05$).

FIG 5 Proposed model for the regulation of PHB synthesis in *B. diazoefficiens* including the possible role of $FixK_2$ (⟶: stimulation; ⟞: inhibition; solid lines indicate transcription; dashed lines depict translation). Permissive conditions, e.g. low O_2, leads to an increase of NADPH and acetyl-CoA concentrations, thus PHB biosynthesis starts using these metabolites as substrates. This biosynthetic process is catalyzed initially by high levels of 3-ketoacyl-CoA thiolase, acetoacetyl-CoA reductase, and PHB synthase due to PhaR sequestration at the PHB granules surface. Meanwhile, *phaC2* expression is stimulated by $FixK_2$, increasing the relative PhaC2/PhaC1 concentration, which progressively decreases total PhaC activity during PHB granules growth. As granules grow, less PHB surface becomes available for PhaR and PhaP, which may provoke a competitive displacement of PhaR by PhaP from the surface, that in turn may repress PhaR-controlled promoters. In the *phaR* mutant, these promoters are not repressed; therefore, PhaP1, PhaP4 and $FixK_2$ levels are increased. Hence, $FixK_2$ stimulates the expression of *phaC2* and the biosynthesis of EPS. Altogether, these changes result in low levels of PHB in the *phaR* mutant. Moreover, in the

722 Δ*phaP1*/Δ*phaP4* strain the very large PHB granule devoid of PhaP1 and PhaP4 may be
723 able to allocate more PhaR than the wildtype at the beginning of PHB biosynthesis. This
724 PhaR sequestration could promote more PHB biosynthetic activity leading to higher
725 PHB accumulation before the PhaC2/PhaC1 ratio reaches its critical value and PhaR
726 begins to accumulate in the cytoplasm. Protein symbols are indicated at the bottom of
727 the Figure. For more details, see text.

Applied and Environmental Microbiology

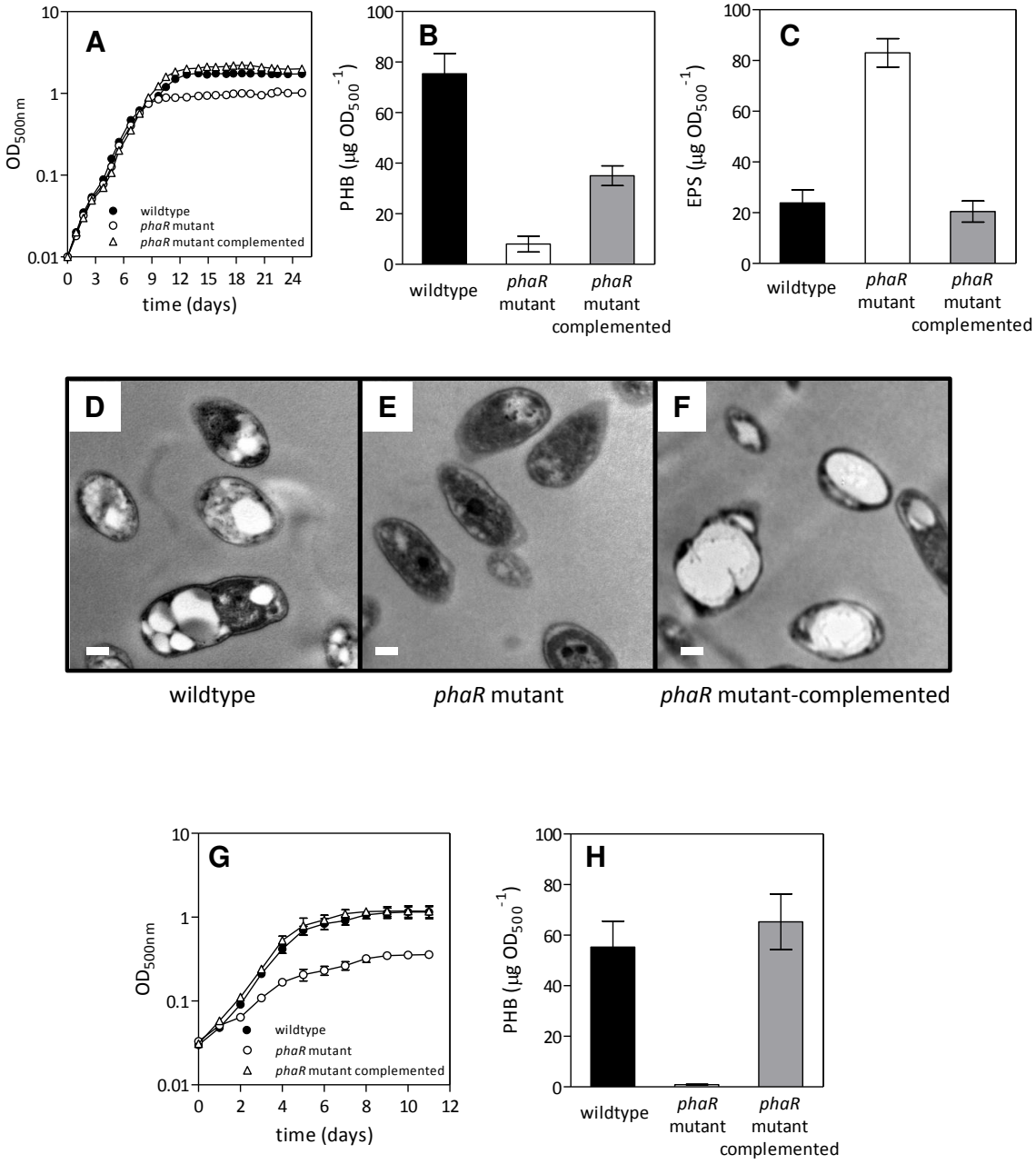

Figure 1

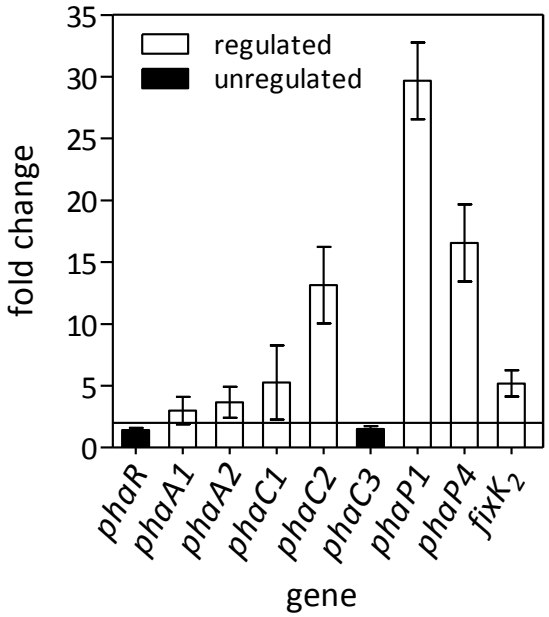

Figure 2

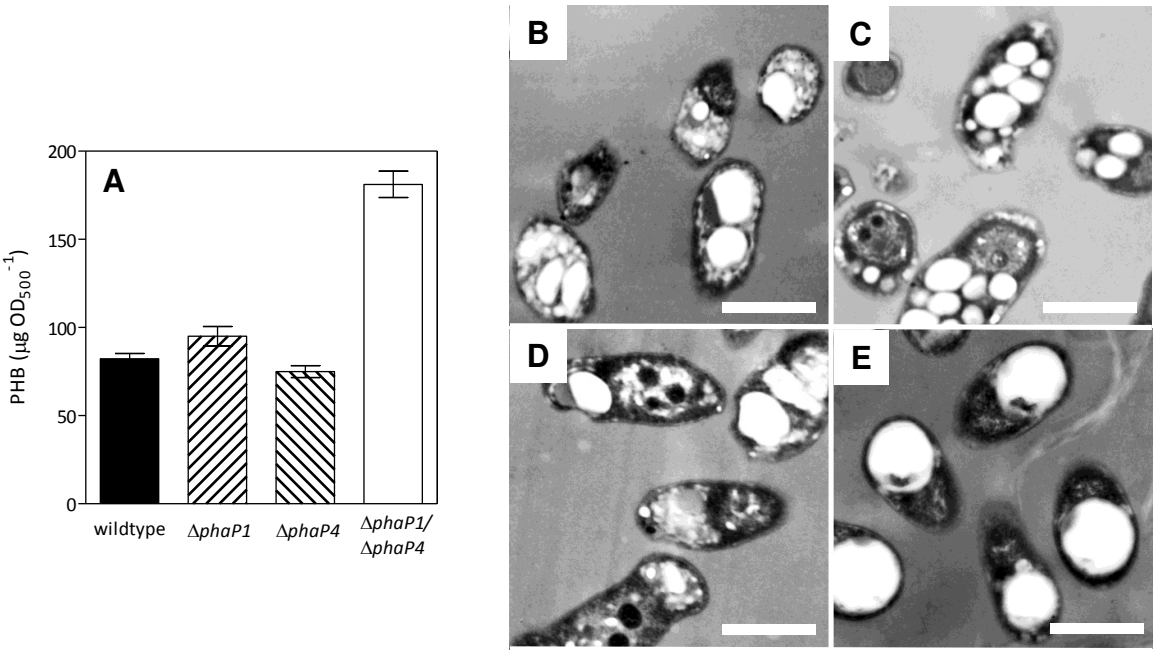

Figure 3

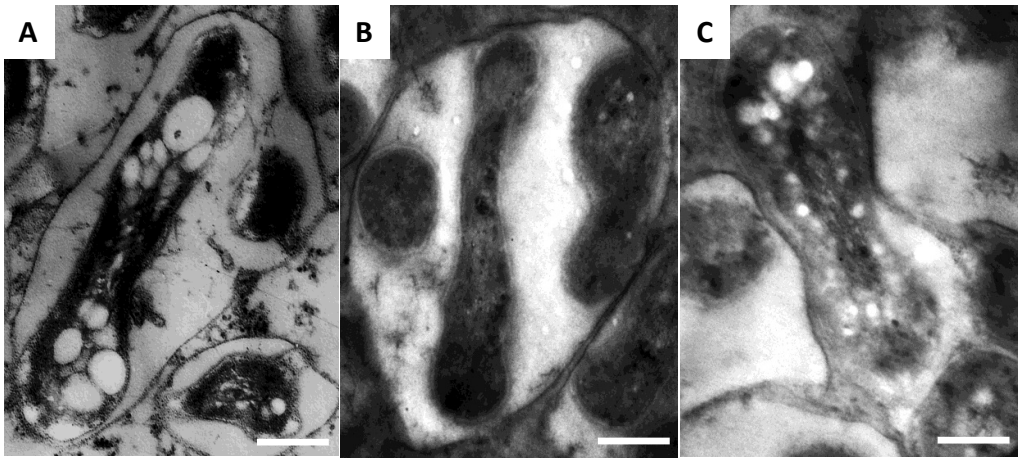

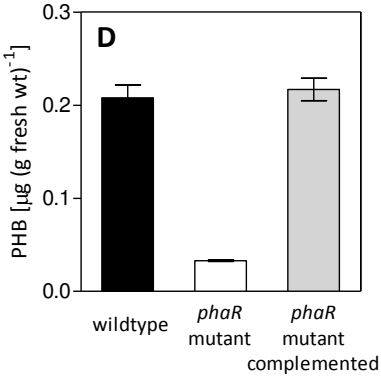

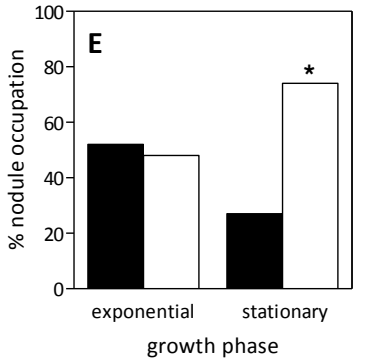

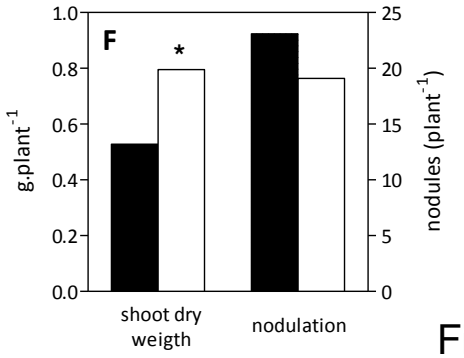

Figure 4

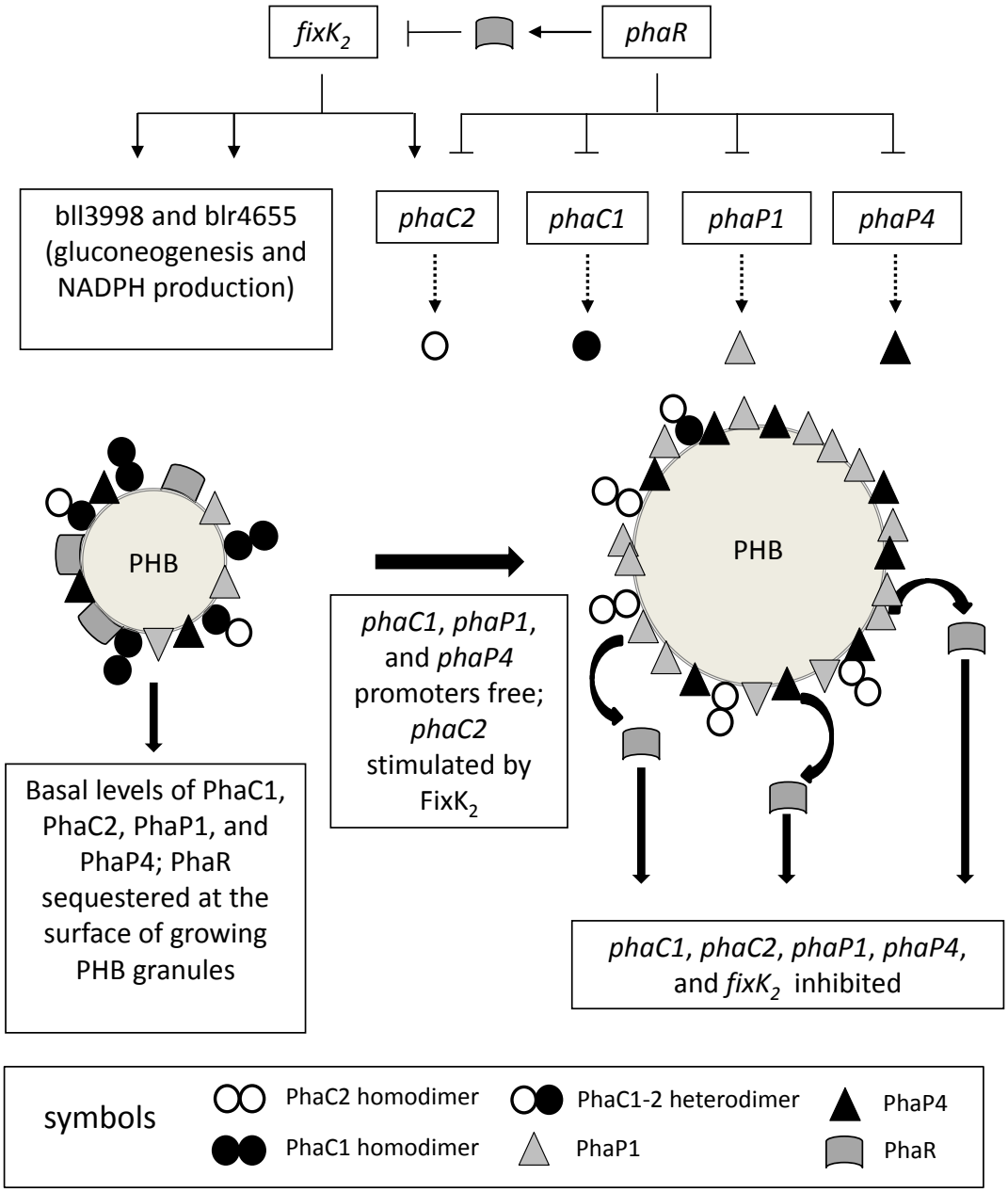

Figure 5